Available online at www.sciencedirect.com
SCIENCE DIRECT®
Biomaterials 26 (2005) 5198–5208
Biomaterials
www.elsevier.com/locate/biomaterials

The enhancement of osteoblast growth and differentiation in vitro on a peptide hydrogel—polyHIPE polymer hybrid material

Maria A. Bokhari[a,b,c], Galip Akay[a,c], Shuguang Zhang[d], Mark A. Birch[b,c,*]

[a]School of Chemical Engineering and Advanced Materials, University of Newcastle, Newcastle upon Tyne, NE1 7RU, UK
[b]School of Surgical and Reproductive Sciences (Orthopaedics), Medical Faculty, University of Newcastle, Newcastle-upon Tyne, NE2 4HH, UK
[c]Institute for Nanoscale Science and Technology, University of Newcastle, Newcastle upon Tyne NE1 7RU UK
[d]Centre for Biomedical Engineering, Massachusetts Institute of Technology, Cambridge, MA 02139-4307, USA

Received 1 September 2004; accepted 17 January 2005

Abstract

The objective of this study was to investigate the effect of combining two biomaterials on osteoblast proliferation, differentiation and mineralised matrix formation in vitro. The first biomaterial has a well-defined architecture and is known as PolyHIPE polymer (PHP). The second biomaterial is a biologically inspired self-assembling peptide hydrogel (RAD16-I, also called *PuraMatrix*^{TM}) that produces a nanoscale environment similar to native extracellular matrix (ECM). Our work investigates the effect of combining RAD16-I with two types of PHP (HA (Hydroxyapatite)-PHP and H (Hydrophobic)-PHP) and evaluates effects on osteoblast growth and differentiation. Results demonstrated successful incorporation of RAD16-I into both types of PHP. Osteoblasts were observed to form multicellular layers on the combined biomaterial surface and also within the scaffold. Dynamic cell seeding and culturing techniques were compared to static seeding methods and produced a more even distribution of cells throughout the constructs. Cells were found to penetrate the scaffold to a maximum depth of 3 mm after 35 days in culture. There was a significant increase in cell number in H-PHP constructs coated with RAD16-I compared to H-PHP alone. Our results show that RAD16-I enhances osteoblast differentiation and indicates that the incorporation of this peptide provides a more permissive environment for osteoblast growth. We have developed a microcellular polymer containing a nanoscale environment to enhance cell: biomaterial interactions and promote osteoblast growth in vitro.

Keywords: Bone tissue engineering; Cell adhesion; Hydrogel; Osteoblast; Osteogenesis; Adhesion mechanism

1. Introduction

There has been a growing interest in developing innovative biomaterials with improved functionality that can be used for biomedical applications and tissue engineering. These scaffolds serve as synthetic extracellular matrix (ECM) to organise cells into a three-dimensional (3D) architecture and to present stimuli, which direct the growth and formation of a desired tissue [1]. The discovery and design of novel biomaterials has become increasingly important for advanced tissue engineering and controlled drug delivery systems [2,3].

We have previously reported that osteoblastic cells preferentially differentiated on hydroxyapatite (HA) modified polymers and produced bone-like tissue [4]. The polymer used in our studies is a porous polymeric foam known as PolyHIPE polymer (PHP), which is fabricated using a high internal phase emulsion (HIPE) polymerisation route producing a structural architecture that can be optimised and modified. We have shown that PHP can support osteoblastic differentiation and

*Corresponding author. School of Surgical; Reproductive Sciences (Orthopaedics), Medical Faculty, University of Newcastle, Newcastle-upon Tyne, NE2 4HH, UK. Tel.: +44 1912 225659; fax: +44 1912 228514.
E-mail address: m.a.birch@ncl.ac.uk (M.A. Birch).

0142-9612/$ - see front matter © 2005 Elsevier Ltd. All rights reserved.
doi:10.1016/j.biomaterials.2005.01.040

bone growth in vitro and determined that while pore size (40–100 μm) does not influence cell differentiation it can influence cell penetration [4]. The flexibility of this polymer, its ease of production, the ability for pore and interconnect sizes to be tailored as required, make it a strong candidate for tissue engineering applications.

Several biomaterials composed of copolymers, synthetic organic polymers and proteins, have been introduced in the last decade. These include hydrogels, a class of hydrated polymer materials (water content $\geqslant 30\%$ by weight) that are being employed as scaffold materials [5] providing a 3D environment for cell growth [6,7]. Such gels can be tailored by incorporation of biologically active molecules such as laminin to improve cell growth [8].

A new class of peptide-based biological materials were discovered in yeast from the study of self-assembling ionic self-complementary peptides [9,10]. The peptides consist of alternating hydrophilic and hydrophobic amino acids and are designated as type I self-assembling peptides (sapeptides, now called *PuraMatrix*^{TM}) because they contain amino acid sequences that facilitate the formation of a hydrogel scaffold with $>99\%$ water content (1–10 mg/ml). These peptides have a motif, RAD, that is similar to the ubiquitous integrin receptor binding site RGD. While it is not known if the RAD repeats behave in the same manner to RGD motifs, their properties as cell adhesion molecules have been studied in several different cell types [11]. Work using these peptide has demonstrated that a variety of cells encapsulated and grown in 3D peptide scaffolds show functional differentiation, active migration, and extensive production of their own extracellular matrices [12,13]. For instance these peptides can be used as a 3D scaffold for the encapsulation of chondrocytes, supporting characteristic spherical morphology and abundant Type II collagen and GAG production [14].

These self-assembling peptides, including RAD16-I, assemble into nanofibers at physiological pH simply by altering NaCl or KCl concentration. Because the resulting nanofibers are 1000-fold smaller than synthetic polymer microfibers, they surround cells in a manner similar to ECM. Moreover, biomolecules in such a nanoscale environment diffuse slowly and are likely to establish a local molecular gradient more closely mimicking the in vivo scenario [15].

Given the strong metabolic demands of osteoblastic cells during mineralised tissue formation, effective nutrient delivery has long been considered an important factor for successful tissue engineering of bone [16]. In studies of osteoblastic cell growth on 3D constructs, studies show preferential short-term growth of osteoblastic cells on exterior regions of scaffolds [4,17]. Therefore, to circumvent possible nutrient transport limitations in static 3D culture and since mechanostimulation is a potent regulator of bone cell behaviour, dynamic culture systems have been developed.

We illustrate in this study the implementation of a novel cell seeding technique and the utilisation of a dynamic cell culturing system to improve cell penetration and growth. In addition, we set out to establish if the combination of RAD 16-I peptide hydrogel with HA-PHP or H-PHP provides an enhanced microenvironment in which cells are able to attach, proliferate and maintain their osteoblastic phenotype compared to PHP alone. The integration of these two biomaterials and a dynamic spinner cell culture system should provide an excellent environment to encourage bone growth on a 3D support in vitro.

2. Materials and Methods

2.1. Preparation of PolyHIPE scaffold (PHP) and of PHP-RAD 16-I constructs

We have previously described in detail the preparation and fabrication of PHP [4]. Briefly PHP foams were prepared using the polymerisation of a HIPE as described by Akay et al. [18]. The pore size used for this study was 100 μm which was determined at the HIPE stage. The oil phase contained 78% Styrene, 8% DVB monomer (cross-linking agent) and 14% Span 80 surfactant, sorbitan monooleate. Two types of PHP were manufactured and these differed in the composition of the aqueous phase. For polymers modified with hydroxyapatite (HA-PHP) their aqueous phase contained 1% potassium persulphate, 0.5% HA and 15% phosphoric acid. Polymers without hydroxyapatite (H-PHP) had an aqueous phase consisting of 1% potassium persulphate only. Emulsification was carried at 80 °C to achieve a pore size of 100 μm and the volume fraction of the internal phase used was 95%. The processing conditions were RD (dosing rate of the aqueous phase) $= 1.77$ ml/s, impeller speed, $'\Omega = 300$ rpm. After emulsification, the HIPE was transferred to cylindrical containers (26 mm internal diameter) and polymerised at 60 °C for 8 h. PHP samples were cut into discs, 26 mm in diameter and 3 mm in thickness.

To prepare PHP scaffolds for cell culture, the PHP discs were washed in isopropanol and then with dH_2O in a Soxhlet system. Polymer samples were finally dried in a vacuum oven and then sterilised.

2.2. Peptide design and synthesis

The synthesis and characterisation of RAD16-I has been described previously [13]. Briefly the peptide RAD16-I with the sequence AcN-RADARADARA-DARADA-CNH_2 was synthesised (Sigma, Genosys) to $>70\%$ purity. RAD16-I was dissolved in 100 μl DMSO

and then made up with 295 mM sucrose solution at a peptide concentration of 10 mg/ml. The sucrose solution was found to be a suitable medium for peptide dissolution and subsequent self-assembly.

2.3. Cell isolation and culture

Culture media and supplements were obtained from Invitrogen (Paisley, UK) unless otherwise stated. Primary rat osteoblasts were isolated from neonatal rat calvariae based on methods previously described [19,20]. The collected cells were then grown in Dulbecco's modified Eagle's medium (DMEM) supplemented with 10% fetal calf serum (FCS), 100 μg/ml streptomycin and 100 U/ml penicillin.

2.4. Cell seeding and dynamic culture

Trypsinised primary osteoblasts were resuspended in 2 ml s^{-1} of peptide solution (0.5% (w/v)) at a cell seeding density of 1×10^6 cells/scaffold. The cell-peptide solution was then dynamically seeded onto PHP at a flow rate of 25 μl/min. The flow rate was chosen after preliminary experiments found this to be optimal for seeding large numbers of viable cells in our system. The cell seeding chamber was machined from a 28 mm teflon disc and consists of a cell loading chamber that accommodated the PHP sample, a threaded lid and inlet/outlet ports on either face of the disc. Flow through the chamber was controlled by a syringe pump (pHD 2000 Harvard apparatus).

For cell-peptide seeding, the construct was transferred into PBS to initiate self-assembly. When the peptide is exposed to an electrolyte solution like phosphate buffered saline (PBS) the solution initiates β-sheet assembly into interweaving nanofibers. Such self-assembly occurs rapidly when the ionic strength of the peptide exceeds a certain threshold, or the pH is such that the net charge of the peptide molecules is near zero [10,11]. A cell-peptide control without PHP was also prepared. After 4 h, successful self-assembly occurred, with the formation of a hydrogel and then the $1 \times$ PBS was replaced with DMEM and supplemented with 10% fetal calf serum (FCS), 100 μg/ml streptomycin, 100 U/ml penicillin. The constructs were statically cultured at 37 °C in a humidified atmosphere with 5% CO_2. After 7 days, the cell peptide-PHP constructs were transferred into a spinner flask environment. To encourage differentiation of these cells to an osteoblastic phenotype cultures were supplemented with DMEM, 10% FCS, 5 mmol/l β-glycerophosphate, 100 μg/ml ascorbic acid phosphate and 10 nMol dexamethasone (Sigma). Cell-peptide-PHP constructs were cultured for 35 days in vitro. Media was changed every 4 days.

Cells were statically seeded onto PHP as follows; the discs were immersed in 5 ml of complete culture medium overnight prior to cell seeding. The medium was replaced and 1×10^6 cells were added to the well and the osteoblasts were allowed to settle onto the PHP discs. Each well had a final volume of 5 ml media. All experiments were cultured in appropriate media at 37 °C in a humidified atmosphere with 5% CO_2.

2.5. Preparation of samples for SEM analysis

All constructs for analysis by SEM were fixed in 2% gluteraldehyde/PBS, dehydrated, snap fractured and critical point dried from CO_2 at 38 °C and 1200 psi. Samples were mounted, splutter coated with gold and examined under SEM (Cambridge s240). PHP-RAD 16-I constructs analysed by confocal laser scanning electron microscopy (CLSM) were fixed in 4% paraformaldehye/PBS and incubated with 16 units of phalloidin-TRITC (Sigma) for 30 min at room temperature; in order to visualise the cytoskeleton, and with 4′, 6 diamidine-2′ phenylindole dihydrochloride (DAPI), (Sigma) for approximately 5 min to visualise the nuclei. Specimens were examined with a BioRad MRC-600 CLSM (BioRad Microscience Ltd, IK), equipped with an ion argon laser source and two photomultiplier tubes. Depth projection micrographs were visualised by 20 to 30 horizontal image sections throughout the samples (serial optical section set).

2.6. Analysis of cell-scaffold construct cellularity

The DNA content of the lysates was determined by using a fluorometric DNA assay [21]. Cell-scaffold constructs were lysed by a freeze-thaw method in deionised distilled water (ddH_20). DNA standard curve and study samples were mixed with 1.3 ml of a 200 ng/ml Hoechst 33258 dye (Sigma) in a 100 mM NaCl and 10 mM tris buffer solution. Fluorescence emission was read at 455 nm and cells were excited at a wavelength at 350 nm on a fluorescence spectrophotometer.

2.7. Quantitative measurement of alkaline phosphatase activity in constructs

Cell-scaffold constructs were lysed by a freeze-thaw method in ddH_20. Alkaline phosphatase (ALP) activity was determined by a colorimetric assay kit using the conversion of paranitrophenylphosphate to para-nitrophenol (104-LL Kit, Sigma) which was read at 405 nm on a spectrophotometer. ALP activity was normalised to the total cell number per scaffold for each time point.

2.8. Rat osteopontin ELISA assay

Osteopontin secreted in the culture media was measured using a commercially available sandwich immunoassay specific for rat osteopontin generously

donated by Assay designs (Northampton, UK). The assay is based on two rabbit polyclonal antibodies for rat osteopontin. One antibody is immobilised on a microtiter plate, and the second one is labelled with the enzyme horseradish peroxidase. Undiluted conditioned media was analysed as outlined in the manufacturer's protocol.

2.9. Histological preparation and analysis

Constructs were prepared for histology after 35 days in culture. Samples were fixed in 4% formaldehyde. Following dehydration, samples were paraffin-embedded, sectioned at 7 μm and stained with Haematoxylin and Eosin (H&E) or Von Kossa. For Von Kossa staining, the cells were fixed with 4% paraformaldehyde and stained for mineral deposition. The cells were incubated in 2% silver nitrate in front of a 60 W white light lamp for 1 h and rinsed three times with distilled water. The final fixation was performed with 2.5% sodium thiosulphate for 5 min. Digital images were captured on a light microscope, then analysed using Scion Image for Windows (Freeware). Images from the H&E sections were used to quantify cell penetration with histomorphometric techniques. Three independent sections from each specimen were analysed and the distance of the deepest cell from the PHP surface was determined in five equally spaced regions (each 0.2 mm in width) from three randomly selected fields (1 mm in width) within each section.

2.10. Statistical analysis

The data presented from DNA, ALP and osteopontin assays were collected from three independent experiments for each condition. Student's *t*-test was used to determine the statistical significance. Mann Whitney *U* tests were performed to determine any significant differences in the relationship between cell penetration and culture type.

3. Results

3.1. Dynamic cell seeding improves spatial uniformity

Primary rat osteoblasts were seeded using the dynamic technique onto HA-PHPs. Histological analysis after 7 days in vitro, demonstrated more uniform cell densities throughout the depth and across the polymer (Fig. 1b and c) compared to the static seeding method, where cells accumulated in pockets and some regions inside the construct were essentially void of cells (Fig. 1a). Reinforcing what was seen with the histological analysis, confocal laser scanning microscopy (CLSM) further demonstrated that the use of a dynamic cell seeding method increased the penetration of cells and produced an even distribution of cells throughout the entire scaffold. The depth of penetration was determined for cell-polymer constructs that were statically seeded and constructs that were dynamically seeded. Cells were found to penetrate in dynamically cultured cell-scaffold constructs to a significantly ($p<0.005$) greater depth than cells seeded and cultured in a static environment (Fig. 1d) after 7 and 35 days in vitro. Therefore, all subsequent scaffold constructs were dynamically seeded and cultured.

3.2. PHP-RAD 16-I constructs support cell growth

When the PHP-RAD16-I constructs were examined by SEM it was evident that the peptide had been successfully integrated within the scaffold (Fig. 2a) and found on the surface of PHP throughout each sample. There was evidence of individual interwoven fibres, whose structure was similar to published SEM micrographs of RAD16-I [13]. After 35 days in culture, the cell-peptide-HA-PHP and cell-peptide-H-PHP constructs were also analysed by SEM. Both construct types supported osteoblastic growth (Fig. 2b–d). Cells had formed a confluent layer and there were some regions where cells had aligned in the absence of any obvious topographical cue (Fig. 2b,c). Thick layers of orientated cells were observed and ECM was deposited both on the scaffold surface and within the constructs. Cells within the peptide-H-PHP construct exhibited a more fibroblastic appearance (Fig. 2c) suggesting good cell adhesion, compared to the more rounded cells observed in H-PHP alone (Fig. 2d). Cells cultured on HA-PHP scaffolds adhered well [4] and exhibit similar morphological features to cells on HA-PHP-RAD16-I scaffolds (Fig. 3b and d). On H-PHP scaffolds, there were only sporadic areas of cells although where cells had collected ECM was formed (Fig. 3a). Inclusion of RAD16-I with H-PHP increased the apparent number of cells and cell colonies (Fig. 3c).

3.3. Analysis of cell growth on RAD16-I—PHP scaffolds

Levels of cellular DNA were assessed as a measure of cell number for each of the construct types investigated in this study (Fig. 4a). Analysis of these data showed that proliferation proceeded significantly in HA-PHP scaffolds with or without the inclusion of RAD16-I compared to H-PHP scaffolds ($p<0.01$). There was no statistical significance in cell number when HA-PHP was compared to HA-PHP-RAD16-I constructs. However, the amount of DNA isolated from H-PHP-RAD16-I constructs was significantly more than H-PHPs ($p<0.05$).

Cell growth was quantified by histomorphometric techniques in all constructs studied and viable cells were

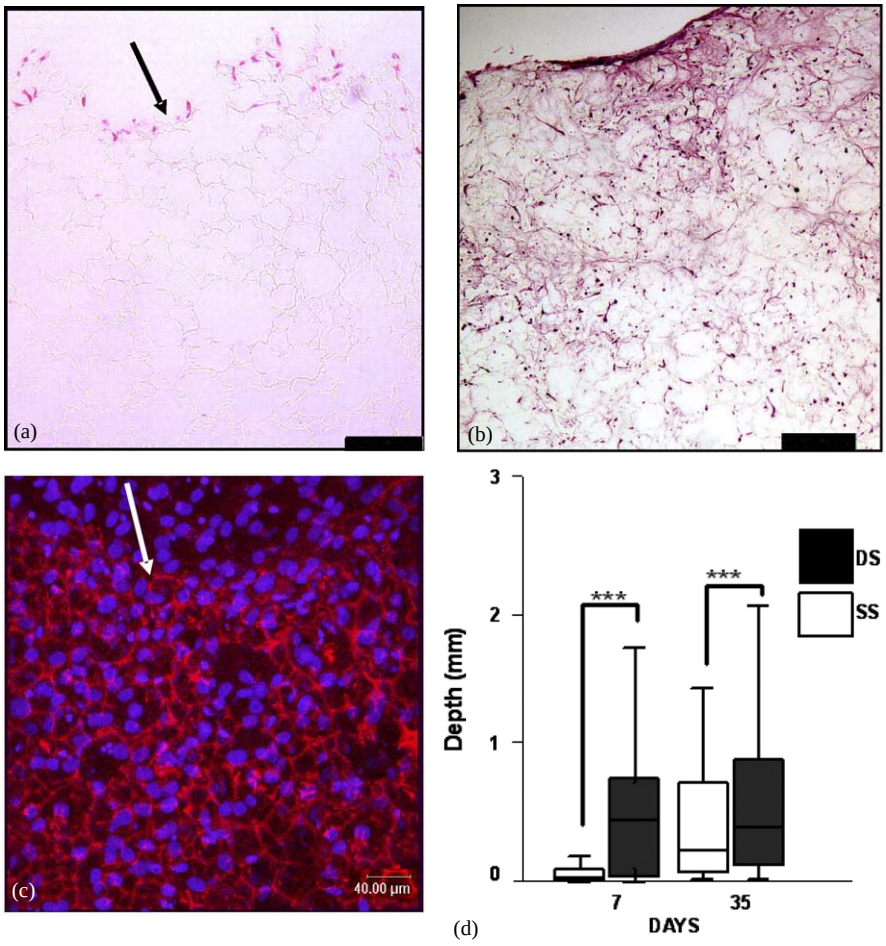

Fig. 1. Haematoxylin and Eosin transverse sections of seeded HA-PHP: (a) cells statically seeded and (b) cells dynamically seeded. Panel (c) shows a CLSM image of a transverse section of cells penetrating PHP in a uniform manner. Cytoskeleton is stained with Rhodamine-phalloidin and the nucleus with DAPI. Arrows indicate the surface of PHP and (d) box plot showing the effect of static seeding and culturing (SS) and dynamically seeding and culturing on the depth of penetration of rat calvarial osteoblasts cultured for 7 and 35 days in vitro. Box plots show the median, quartiles and extreme values. The box represents the interquartile range, which contains 50% of the values. The whiskers are lines that extend from the box to the highest and lowest values, excluding the outliers. The line across the box represents the median value. ***Denotes statistically significant differences between the different seeding and culturing systems used, $p<0.005$.

identified to a maximal depth of 3 mm (Fig. 4b). Cell growth was supported inside HA-PHP more readily compared to H-PHP constructs and this was also observed with the addition of RAD16-I to either polymer type ($p<0.005$). Cell number and penetration was significantly enhanced when RAD16-I was incorporated in HA-PHP constructs ($p<0.01$). The addition of RAD 16-I to H-PHP constructs was found not to have a significant effect on cell penetration.

3.4. Osteoblast differentiation

The ALP activity of osteoblastic cells is an indication of their commitment towards this lineage [22]. The ALP activity of the constructs was normalised by the number of cells per construct (Fig. 5). All PHP constructs were found to express ALP. The presence of RAD16-I resulted in a statistically significant difference in the ALP activity for constructs with either PHP ($p<0.05$). Levels of activity were comparable between the HA and H-PHP RAD 16-I constructs.

Osteopontin is a phosphorylated glycoprotein that is synthesised by osteoblasts and is associated with osteogenesis preceding mineralisation [23]. Osteopontin secreted into the culture media of H-PHP and H-PHP-RAD16-I was measured (Fig. 6) and detected in both types of construct with significant increases observed in H-PHP-RAD16-I constructs ($p<0.005$) at all time points. Osteopontin production increased in a time-dependent fashion ($p<0.005$) for both types of constructs.

Von kossa staining identified areas of mineral deposition indicative of expression of the mature osteoblastic phenotype. Mineralised tissue was present in large areas within the constructs in H-PHP-RAD16-I (Fig. 7c). This is in marked contrast to H-PHP, in which

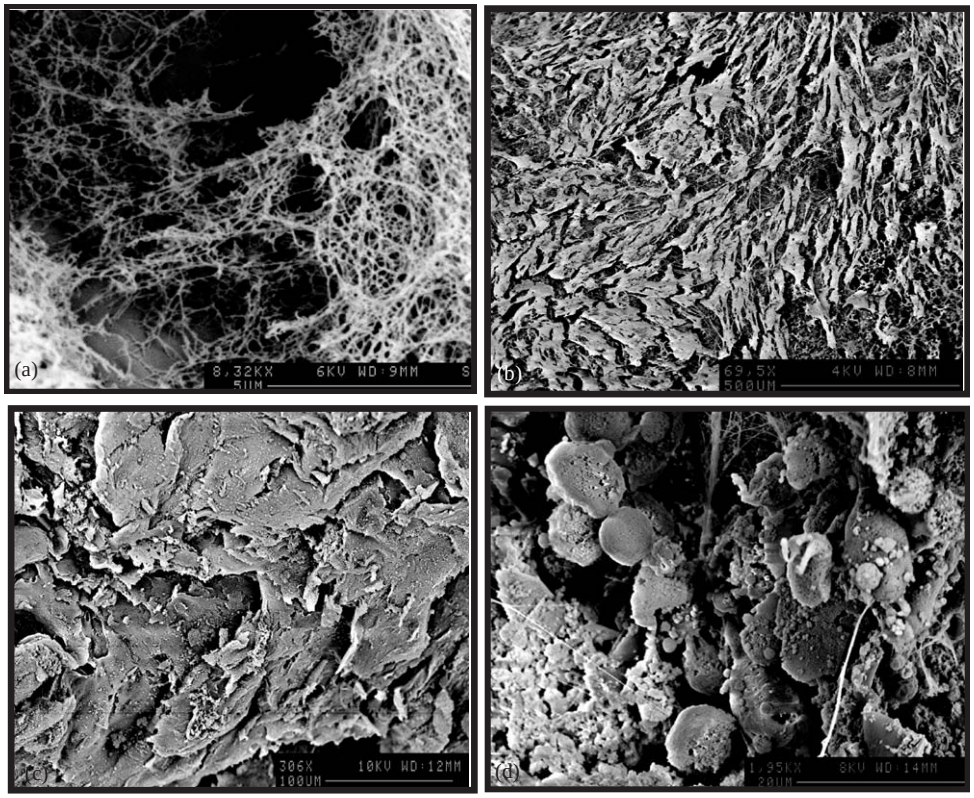

Fig. 2. Scanning electron micrographs (SEM) of the RAD 16-I peptide hydrogel showing (a) RAD 16-I surface. The diameters of the filaments are approximately 10–20 nm and the enclosures between the fibres are approximately 50–100 nm; (b) primary osteoblast growth dynamically seeded and cultured on the surface of HA-PHP-RAD 16-I; (c) shows osteoblast growth on H-PHP-RAD 16-I; (d) illustrates osteoblasts on the surface of H-PHP. Cells for all experiments were cultured for 35 days in vitro.

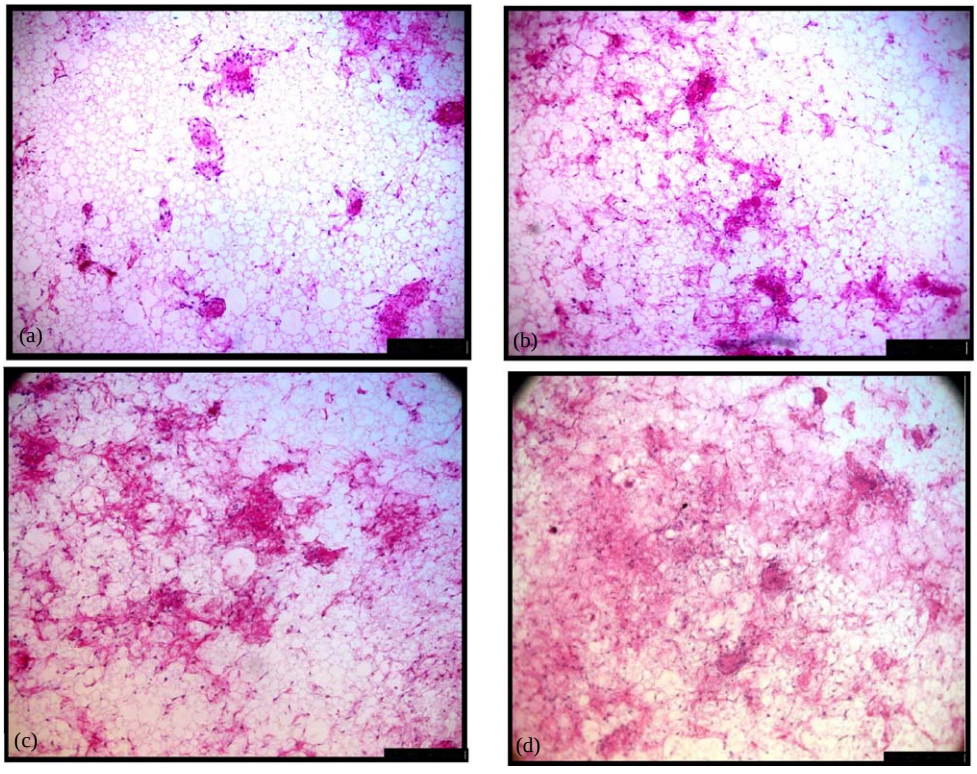

Fig. 3. Haematoxylin and Eosin surface sections of primary rat osteoblasts cultured on H-PHP and HA-PHP with/without the incorporation of RAD 16-I at 35 days in vitro: (a) H-PHP alone, (b) HA-PHP alone, (c) H-PHP-RAD 16-I and (d) shows cells cultured on HA-PHP-RAD 16-I. Scale bar = 0.1 mm.

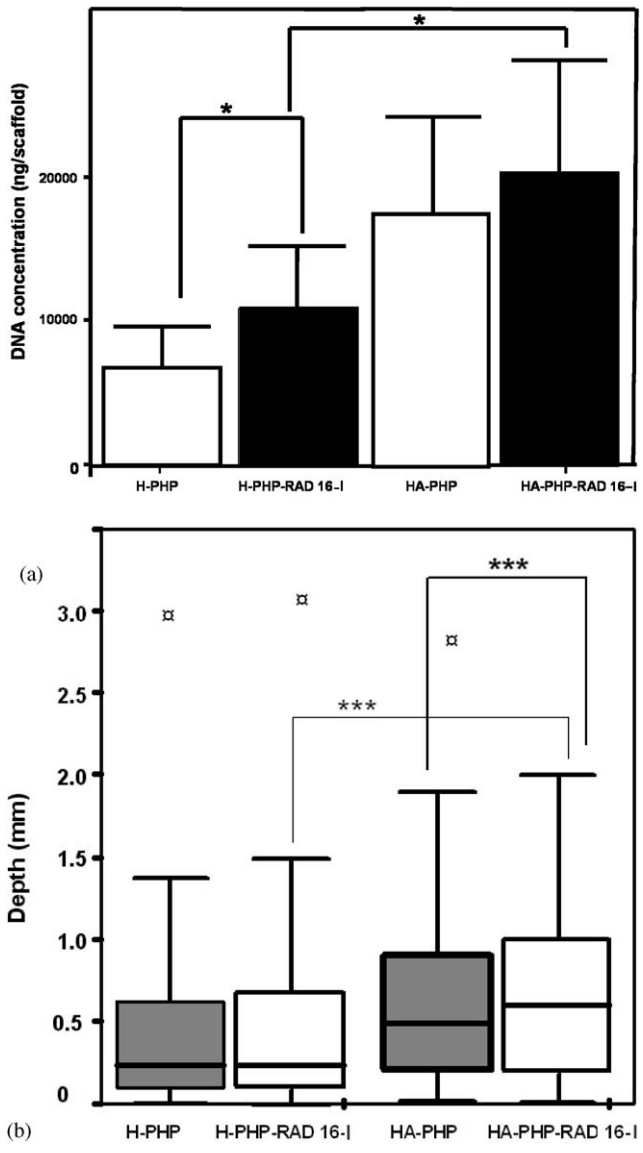

Fig. 4. (a) The effect of combining RAD 16-I with HA-PHP or H-PHP on cell number. DNA content was measured after 35 days. Each bar represents the mean ($n = 3$) $\pm$SD. Statistical significance was determined by student's t-test, where $p < 0.01$ (**). (b) Depth of osteoblast penetration from the surface of the biomaterial combinations. Cells were dynamically seeded and cultured in a spinner environment for 35 days in vitro on H-PHP or HA-PHP with or without the addition of RAD 16-I. The box represents the interquartile range which contains 50% of the values. The whiskers are lines that extend from the box to the highest and lowest values. The line across the box indicates the median. Extreme values are denoted (¤). Statistical significance was determined by the students t-test where $p < 0.005$***.

only the surface appeared to show any mineralisation. HA-PHP-RAD16-I (Fig. 7d) showed mineral deposition throughout the sections, whereas in HA-PHP mineralisation was observed sporadically within the constructs (Fig. 7b).

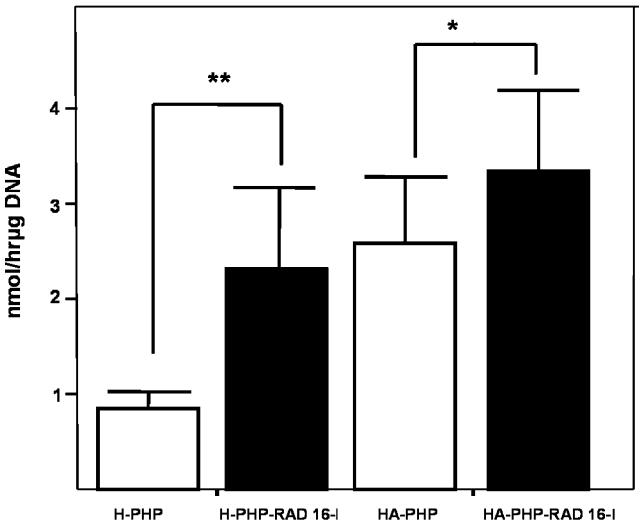

Fig. 5. Bar chart showing the effect of the combination of PHP and RAD 16-I on the alkaline phosphatase activity of primary rat osteoblasts cultured on HA-PHP and H-PHP for 35 days in vitro. Each bar represents the mean ($n = 3$) $\pm$SD. Statistical significance was determined by the students t-test, where $p < 0.05$ *, $p < 0.01$.

4. Discussion

In tissue engineering, the microenvironment provided by the scaffold must support cell attachment; proliferation and differentiation; neo tissue generation and correct 3D organisation. One approach towards ideal scaffold design is through biomimetic methodology [24], using the modification of biomaterials with bioactive molecules. For example, the modification of scaffolds with peptide sequences can facilitate cellular functions such as adhesion, proliferation and migration [3,24].

Recent studies have demonstrated the potential of combining materials with bioactive molecules, for example the generation of poly D, L-lactic acid (PLA) films coupled with adhesion peptide sequences linked to poly (L-lysine) (PLL) promote attachment of endothelial cells and modulation of human osteoprogenitor activity [26,27]. It has also been observed that peptide-modified polymers demonstrate enhanced initial cell attachment and a significant increase in parameters reflecting the osteoblastic phenotype [27,28].

In this study, RAD16-I was used in conjunction with PHP, to produce a hybrid material with a controlled biosurface and micro-scale features (pores, interconnects). RAD16-I possesses unique features making it an exciting tissue engineering material. The peptide scaffold spontaneously self-assembles into nanofibers (i.e. 10–20 nm in diameter) that are highly hydrated, trapping water at total volume contents of 99.5%. In such a "nanofiber scaffold", cells are embodied in a truly 3D environment [25]. We hypothesised that the combination of RAD16-I and PHP would enhance osteoblast

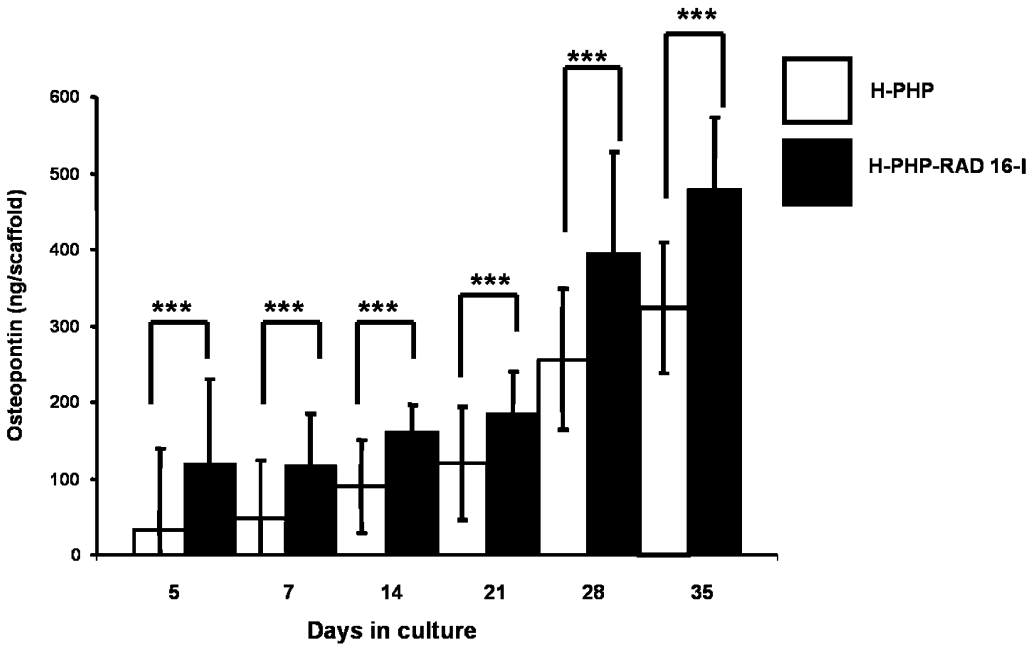

Fig. 6. Osteopontin secretion from H-PHP and H-PHP-RAD 16-I constructs. Results are expressed as nanogram (ng) of osteopontin per scaffold. Each bar represents the mean ($n = 3$) $\pm$SD. Statistical significance was determined by the students t-test, where ***$p < 0.005$.

growth and function by providing a more favourable biomaterial microenvironment.

As well as biomaterial selection and optimisation, cell seeding is also an important step in the in vitro cultivation of engineered tissues. Optimisation of cell seeding is therefore an essential component for the success of in vitro cultivation of large tissue constructs. Cell seeding of scaffolds should result in good cell adhesion, growth and finally a spatially even distribution of attached cells, to provide a basis for uniform tissue regeneration within the scaffold [29]. We have shown in previous work that when cells are statically seeded onto PHP a dense layer of cells accumulate on the surface compared to within the scaffold. Although many cells are found within the construct at early time points and cells migrate within the scaffold over time, most remain localised to the upper surface of PHP. It is therefore likely that since the transport of low molecular weight metabolites, waste products and other macromolecules within a statically seeded scaffold results primarily from diffusion, cells tend to stay at the surface of the scaffold where nutrient availability is high. Therefore, to circumvent possible nutrient transport limitations and to maintain a uniform distribution of cells within the scaffold, we developed a dynamic cell seeding and culture system in this study.

Our data shows that this system improved the distribution of cells within the scaffold. Cells were seen to grow throughout the polymer and the cells remained viable during the 35 days in vitro, indicating that cells were appropriately exposed to nutrients deep within the scaffold. This is likely due to the hydrodynamic stresses created in spinner flasks causing fluid flow across the external surfaces which in turn form eddies around the scaffold thereby improving nutrient transport into the pores [30]. This system therefore offers a promising approach although a disadvantage is the degree of manipulation that is required to transfer the construct from one system to another during the culture period. Flow perfusion seeding and culture of cells all in one bioreactor is being developed, both potentially avoiding the risk of contamination and providing fluid flow-induced mechanical stimulation [30,31].

In our study, two types of PHP (H-PHP and HA-PHP) were investigated with RAD16-I. H-PHP that provides an environment for osteoblast growth in which osteoblast differentiation is delayed [4]. We showed previously that modification of PHP with HA resulted in more cells penetrating and migrating within the polymer. These observations are in agreement with the work of others that shows that HA improves osteoconductivity. Data presented here assesses whether the combination of RAD16-I with PHP enhances the scaffolds properties to provide a suitable microenvironment for osteoblast growth and proliferation.

Our results demonstrate that the combination of RAD16-I and PHP significantly increase the depth at which cell growth is supported in HA-PHP constructs at 35 days. This observation was not repeated for H-PHP-RAD16-I constructs. Although, seeding cells in RAD16-I did result in an increase in overall cell numbers for both types of PHPs. It is likely that the stimulus for

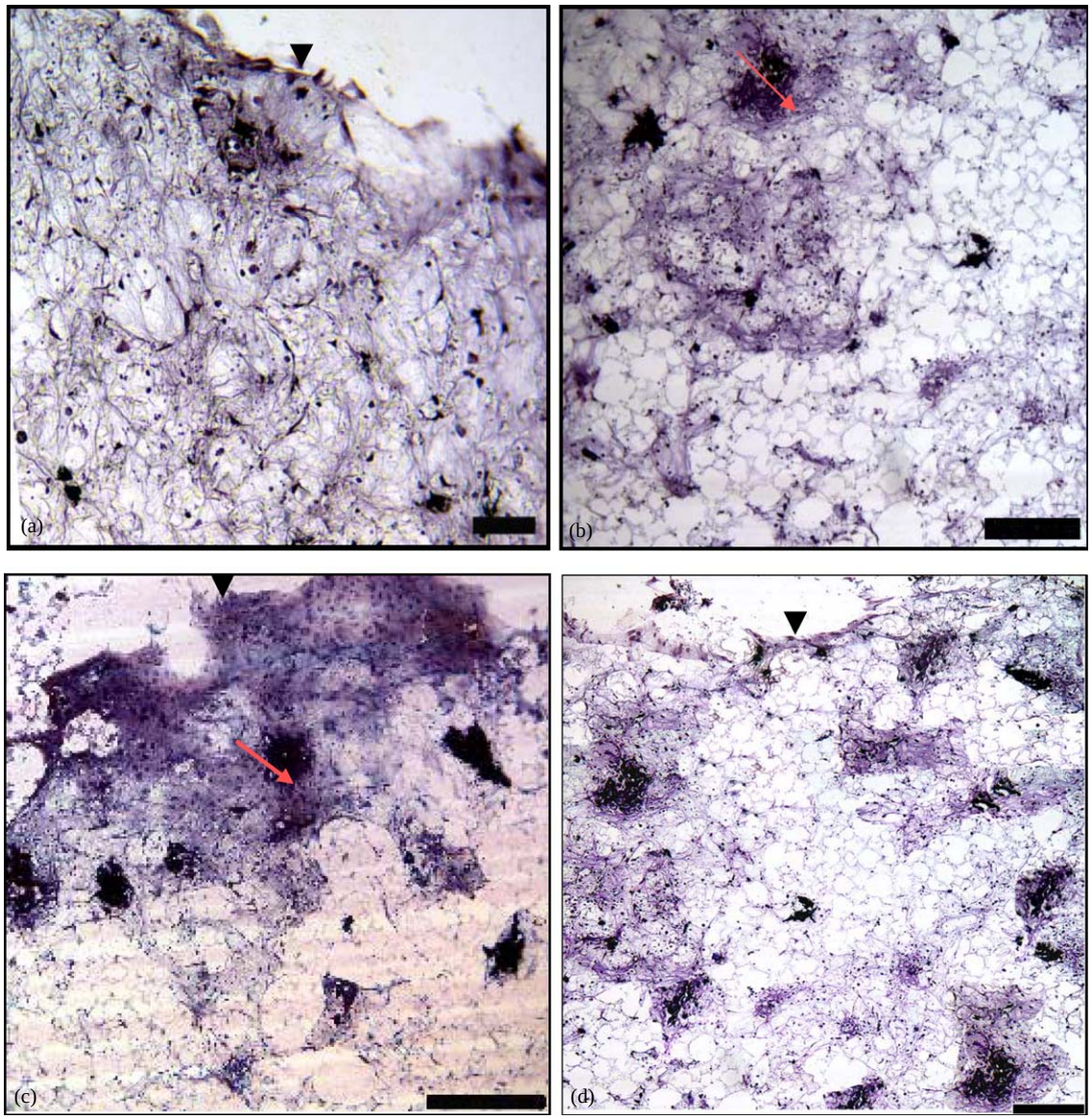

Fig. 7. Von Kossa staining showing transverse sections of primary osteoblast cells on HA-PHP and H-PHP with or without the incorporation of RAD 16-I after 35 days in vitro: (a) H-PHP, (b) HA-PHP, (c) H-PHP-RAD 16-I and (d) HA-PHP-RAD 16-I. Scale bar = 0.1 mm. The intensely stained black areas represent bone nodules forming. Red arrows indicate the bone-like nodules and black arrows indicate the upper surface of the biomaterial.

increased cell numbers and growth observed in RAD 16-I treated constructs is due to the ability of cells to attach more firmly in this environment. RAD16-I is believed to mimic RGD peptides and therefore provide a suitable biological cue to promote cell adhesion and proliferation, thereby rendering the intrinsically less adhesive H-PHP, cell adhesive and enhancing this construct for cell growth. The SEM data shows H-PHP-RAD16-I constructs supported osteoblast morphology in a comparable manner to cells on HA-PHP constructs, with elongated fibroblastic-type cell shape contrasted with the rounded cellular morphology observed in plain H-PHP constructs (Fig. 2d). The physio-chemical difference between hydrophobic, H-PHP and surface-modified HA-PHP may influence the stability of the interface between RAD 16-I and the polymer which in turn could account for the differences in cell behaviour observed in this study. Cells grew preferentially on PHP-RAD16-I constructs, although there was no statistical difference observed between HA-PHP and HA-PHP-RAD16-I constructs (Figs. 3 and 4). This therefore suggests that HA-PHP constructs already provide a suitable micro-environment for osteoblast growth and differentiation.

Cells cultured on H-PHP-RAD16-I showed elevated ALP activity and osteopontin production compared to osteoblasts cultured on H-PHP alone. Von Kossa

stained nodules were also more abundant and observed throughout transverse sections of PHP with RAD 16-I. This study therefore demonstrates that mineralisation is likely to be influenced by the immobilisation of the RAD16-I peptide, creating an environment more permissive for osteoblast adhesion, differentiation and bone formation.

In summary, this work indicates that the combination of RAD16-I and H-PHP promotes improved cell adhesion and differentiation of osteoblastic cells. These findings suggest that the combination of these two unique biomaterials has the potential to generate osteoconductive surfaces within a porous scaffold. The successful generation of a 3D biomimetic scaffold incorporating RAD16-I illustrates its potential to support bone formation by exploiting cell-matrix interactions. Furthermore RAD16-I and hydrophobic biomaterials can be combined to improve cell interactions and tissue responses.

5. Conclusion

We have investigated the potential of combining two biomaterials to provide a more permissive environment for cell proliferation and differentiation. This study has demonstrated that PolyHIPE polymer (PHP) in combination with RAD16-I is capable of supporting cell growth and differentiation in vitro. Incorporating RAD16-I with H-PHP significantly increased the ability of this construct to support osteoblast activity and bone formation in vitro compared to H-PHP alone. This study also reveals the benefits of using a dynamic system to seed and culture cells in vitro to provide a uniform distribution of cells within the construct as well as to enhance nutrient transport thereby allowing osteoblasts deep within the scaffold to continually deposit mineralised matrix.

Acknowledgments

This work was funded by the Engineering and Physical Sciences Research Council, UK.

References

[1] Yang S, Leong K-F, Du Z, Chua C-K. The design of scaffolds for use in tissue engineering. Part 1. Traditional factors. Tissue Eng 2001;7:679–89.
[2] Peppas NA, Langer RS. New challenges in biomaterials. Science 1994;263:1715–20.
[3] Shin H, Jo S, Mikos AG. Biomimetic materials for tissue engineering. Biomaterials 2003;24(4):353–4364.
[4] Akay G, Birch MA, Bokhari MA. Microcellular PolyHIPE polymer supports osteoblast growth and bone formation in vitro. Biomaterials 2004;25:3991–4000.
[5] Park JB, Lakes RS. Biomaterials: an introduction. 2nd ed. New York: Plenum Press; 1992.
[6] Blackshaw SE, Arkison C, Davis CJA. Promotion of regeneration and axon growth following injury in an invertebrate nervous by the use of three-dimensional collagen gels. Proc Roy Soc Lond 1997;264:657–61.
[7] Dillon GP, Yu Wm Sridhan JP, Ranieri RV, Bellamkonda RV. The influence of physical structure and charge on neurite extension in a 3D hydrogel. J Biomater Sci 1998;9:1049–69.
[8] Yu X, Dillon GP, Bellamkonda RB. A Laminin and nerve growth factor-laden three-dimensional scaffold for enhanced neurite extension. Tissue Eng 1999;5:291–304.
[9] Zhang S, Lockshin C, Herbert A, Winer E, Rich A. Zuotin, a putative Z-DNA binding protein in *Saccharomyces cerevisae*. EMBO J 1992;11:3787–96.
[10] Zhang S, Holmes TC, Lockshin C, Rich A. Spontaneous assembly of a self complementary oligopeptide to form a stable macroscopic membrane. Proc Natl Acad Sci USA 1993;90:3334–8.
[11] Zhang S, Holmes T, DiPersio M, Hynes RO, Su X, Rich A. Self-complementary oligopeptide matrices support mammalian cell attachment. Biomaterials 1995;16:1385–93.
[12] Zhang S. Fabrication of novel biomaterials through molecular self-assembly. Nat Biotechnol 2003;21:1171–8.
[13] Holmes TC, Lacalle SD, Su X, Liu G, Rich A, Zhang S. Extensive neurite outgrowth and active synapse formation on self assembling peptide scaffolds. Proc Natl Acad Sci USA 2000;97:6728–33.
[14] Kisiday J, Jin M, Kurz B, Hung H, Semino C, Zhang S, Grodzinsky AJ. Self-assembling peptide hydrogel fosters chondrocyte extracellular matrix production and cell division: implications for cartilage tissue repair. Proc Natl Acad Sci USA 2002;99:9996–10001.
[15] Zhang S. Beyond the Petri dish. Nat Biotechnol 2004;22:151–2.
[16] Botchwey EA, Dupree MA, Pollack SR, Levine EM, Laurencin CT. Tissue engineered bone: Measurement of nutrient transport in three dimensional matrices. J Biomed Mater Res 2003;67A:357–67.
[17] Shea LD, Smiley E, Bonadio J, Mooney DJ. DNA delivery from polymer matrices for tissue engineering. Nat Biotechnol 1999;17:551–4.
[18] Akay G, Price VJ, Downes S. Microcellular polymer materials as cell growth media and novel polymers, EP 1183328 A2, 2002.
[19] Bellows CG, Aubin JE, Heersche JNM, Antosz ME. Mineralised bone nodules formed in vitro from enzymatically released rat calvaria populations. Calcif Tissue Int 1986;38:143–54.
[20] Malaval L, Modrowski D, Gupta AK, Aubin JE. Cellular expression of bone-related proteins during in vitro osteogenesis in rat bone marrow stromal cell cultures. J Physiol 1994;158:555–72.
[21] West DC, Sattar A, Kumar S. A simplified in situ solubilization procedure for the determination of DNA and cell number in tissue cultured mammalian cells. Anal Biochem 1985;147:289–95.
[22] Lian JB, Stein GS. Concepts of osteoblast growth and differentiation: basis for modulation of bone cell development and tissue formation. Crit Rev Oral Bio Med 1992;3:269–305.
[23] Denhartdt DT, Guo X. Osteopontin: a protein with diverse functions. FASEB J 1993;7:1475–82.
[24] Woo KM, Chen VJ, Ma PX. Nano-fibrous scaffolding architecture selectively enhances protein absorption contribution to cell attachment. J Biomed Mater Res 2003;67A:531–7.
[25] Semino C, Merok JR, Crane GG, Panagiotakos G, Zhang S. Functional differentiation of hepatocyte-like spheroid structures

from putative liver progenitor cells in three-dimensional peptide scaffolds. Differentiation 2003;71:262–70.

[26] Yang S, Leong K-F, Du Z, Chua C-K. The design of scaffolds for use in tissue engineering. Part 1. Traditional factors. Tissue Eng 2001;7:679–89.

[27] Yang XB, Roach HI, Clarke NM, Howdle SM, Quirk R, Shakesheff KM, Oreffo RO. Human osteoprogenitor growth and differentiation on synthetic biodegradable structures after surface modification. Bone 2003;29:523–31.

[28] Sofia S, McCarthy MB, Gronowicz G, Kaplan DL. Functionalised silk-based biomaterials for bone formation. J Biomed Mater Res 2001;54:139–48.

[29] Van den Dolder J, Spauwen PH, Mikos AG, Jansen JA. Evaluation of various seeding techniques for culturing osteogenic cells on titanium fiber mesh. Tissue Eng 2003;9: 315–25.

[30] Goldstein AS, Juarez TM, Helmke CD, Gustin MC, Mikos AG. Effect of convection on osteoblastic cell growth and function in biodegradable polymer foam scaffolds. Biomaterials 2001;22: 1279–88.

[31] Hoffmann A, Konrad L, Gotzen L, Printz H, Ramaswamy A, Hofmann C. Bioengineered human bone tissue using autologenous osteoblasts cultured on different biomatrices. J Biomed Mater Res 2003;67A:191–9.